Comprehensive Genome-Wide Analysis of the *Aux/IAA* Gene Family in *Eucalyptus*: Evidence for the Role of *EgrIAA4* in Wood Formation

Hong Yu[1], Marçal Soler[1], Hélène San Clemente[1], Isabelle Mila[2,3], Jorge A.P. Paiva[4,5], Alexander A. Myburg[6], Mondher Bouzayen[2,3], Jacqueline Grima-Pettenati[1,*] and Hua Cassan-Wang[1]

[1]*LRSV Laboratoire de Recherche en Sciences Végétales, UMR5546, Université Toulouse III, UPS, CNRS, BP 42617, Auzeville, F-31326 Castanet Tolosan, France*
[2]*Université de Toulouse, INP-ENSA Toulouse, Génomique et Biotechnologie des Fruits, Avenue de l'Agrobiopole BP 32607, F-31326 Castanet-Tolosan, France*
[3]*INRA, UMR990 Génomique et Biotechnologie des Fruits, Chemin de Borde Rouge, F-31326 Castanet-Tolosan, France*
[4]*Instituto de Investigação Científica e Tropical (IICT/MNE), Palácio Burnay, Rua da Junqueira, 30, 1349-007 Lisboa, Portugal*
[5]*IBET – Instituto de Biologia Experimental e Tecnológica, Apartado 12, 2781-901 Oeiras, Portugal*
[6]*Department of Genetics, Forestry and Agricultural Biotechnology Institute (FABI), Genomics Research Institute (GRI), University of Pretoria, Private Bag X20, Pretoria, 0028, South Africa*

*Corresponding author: Email, grima@lrsv.ups-tlse.fr

Abstract

Auxin plays a pivotal role in various plant growth and development processes, including vascular differentiation. The modulation of auxin responsiveness through the auxin perception and signaling machinery is believed to be a major regulatory mechanism controlling cambium activity and wood formation. To gain more insights into the roles of key *Aux/IAA* gene regulators of the auxin response in these processes, we identified and characterized members of the *Aux/IAA* family in the genome of *Eucalyptus grandis*, a tree of worldwide economic importance. We found that the gene family in *Eucalyptus* is slightly smaller than that in *Populus* and Arabidopsis, but all phylogenetic groups are represented. High-throughput expression profiling of different organs and tissues highlighted several *Aux/IAA* genes expressed in vascular cambium and/or developing xylem, some showing differential expression in response to developmental (juvenile vs. mature) and/or to environmental (tension stress) cues. Based on the expression profiles, we selected a promising candidate gene, *EgrIAA4*, for functional characterization. We showed that *Egr*IAA4 protein is localized in the nucleus and functions as an auxin-responsive repressor. Overexpressing a stabilized version of *Egr*IAA4 in Arabidopsis dramatically impeded plant growth and fertility and induced auxin-insensitive phenotypes such as inhibition of primary root elongation, lateral root emergence and agravitropism. Interestingly, the lignified secondary walls of the interfascicular fibers appeared very late, whereas those of the xylary fibers were virtually undetectable, suggesting that *EgrIAA4* may play crucial roles in fiber development and secondary cell wall deposition.

Key words: *Aux/IAA*, Auxin, *Eucalyptus*, Gene expression, Secondary cell walls, Wood formation

Introduction

The plant hormone auxin plays an important role in regulating plant growth and developmental processes such as embryogenesis, apical dominance, lateral root formation, tropism, fruit development and vascular differentiation (Friml 2003). Auxin also plays a crucial role in specifying vascular stem cells (Miyashima et al. 2013), and regulating the activity of the vascular cambium (for a review, see Bhalerao and Fischer 2014)—a lateral meristem that contributes to secondary radial growth of wood in trees. Measurements of auxin levels across wood-forming tissues revealed a radial auxin concentration gradient where high auxin concentrations localize to the cambium, intermediate concentrations to the xylem elongation zone and low concentrations to the maturation zone (Uggla et al. 1996, Tuominen et al. 1997, Uggla et al. 1998). It was proposed that this gradient regulates cambial activity and differentiation of cambial derivatives by providing positional information to cells within the tissue (Uggla et al. 1998, Sundberg et al. 2000, Schrader et al. 2003); however, the hypothesis that auxin acts as a morphogen still lacks strong experimental support (Nilsson et al. 2008, Bhalerao and Fischer 2014). Moreover, the expression patterns of most of the auxin-responsive genes correlate only weakly with auxin concentration across the wood-forming gradient, arguing against a strong and direct impact of auxin levels on radial patterning (Nilsson et al. 2008). In addition, there is only subtle variation in the absolute auxin levels between active and dormant cambium in trees, suggesting that there may be instead a seasonal fluctuation of auxin sensitivity (Uggla et al. 1996, Uggla et al. 2001, Schrader et al. 2003, Schrader et al. 2004). Indeed, the reduced auxin responsiveness of the dormant cambium correlates with reduced expression levels of components of the auxin perception machinery, implying that auxin signaling controls cambial activity by modulation of auxin responsiveness (Baba et al. 2011).

Wood is a highly variable material that is both developmentally and environmentally regulated (Plomion et al. 2001). For instance, in reaction to mechanical stress, a local increase in cambial cell division induces the formation of tension wood in the upper side of bent angiosperm tree stems. Tension wood has specific anatomical features such as the presence of a characteristic inner gelatinous cell wall layer (G layer) (Timell 1969, Pilate et al. 2004). Auxin is proposed to be implicated in the tension response, and application of either exogenous auxin or auxin transport inhibitors is known to induce the formation of G fibers (Morey and Cronshaw 1968, Mellerowicz et al. 2001). For many years it was assumed that auxin distribution is involved in the regulation of tension wood but Hellgren et al. (2004) showed that auxin levels were homogeneously balanced under gravitational stress in bent *Populus* stems. Auxin may instead exert its influence by means of components of its signaling pathway, as suggested by changes in expression of a large set of auxin-related genes (Andersson-Gunneras et al. 2006) including some members of the aspen *Aux/IAA* gene family (Moyle et al. 2002, Paux et al. 2005).

The perception and signaling of auxin involves central regulators such as the transport inhibitor response 1 (TIR1)/auxin signaling F-box (ABFs) proteins, auxin/IAA (Aux/IAA) proteins and auxin response factor (ARF) proteins (Mockaitis and Estelle 2008, Calderon Villalobos et al. 2012). Aux/IAA proteins are direct targets of TIR1 and of its paralogous AFBs (Dharmasiri et al. 2005, Kepinski and Leyser 2005, Tan et al. 2007). At low intracellular auxin concentrations, Aux/IAA proteins act as transcriptional repressors of auxin-mediated gene expression by interacting and sequestering ARF proteins, thus preventing them from regulating the transcription of their target genes (Guilfoyle and Hagen 2007). In contrast, high intracellular auxin levels foster interactions between Aux/IAA proteins and TIR1 E3 ubiquitin–ligase complexes, resulting in the degradation of Aux/IAA proteins by the 26 S proteasome (Gray et al. 2001, Woodward and Bartel 2005, Tan et al. 2007). As a consequence, ARF proteins are released from their Aux/IAA interaction partners and can regulate the transcription of their auxin-responsive target genes.

The *Aux/IAA* genes were first identified in soybean and pea and were described as early auxin-responsive genes (Walker and Key 1982, Theologis et al. 1985, Ainley et al. 1988). This plant-specific transcription factor family has 29 members in Arabidopsis (Overvoorde et al. 2005), the vast majority of which encode short-lived nuclear proteins. Canonical Aux/IAA contains four highly conserved domains (called I, II, III and IV). Domain I contains a conserved leucine repeat motif (LxLxLx) similar to the EAR (ethylene-responsive element-binding factor-associated amphiphilic repression) motif, which is responsible for the transcriptional repressor activity of this protein family (Tiwari et al. 2004) and can also interact with the co-repressor TOPLESS (Szemenyei et al. 2008). Domain II has a motif of five highly conserved amino acids (VGWPP) that leads to the rapid degradation of Aux/IAA proteins through interaction with a component of the TIR1/AFBs ubiquitin–proteasome protein degradation pathway (Gray et al. 2001, Dharmasiri et al. 2005, Kepinski and Leyser 2005). This interaction is abolished by mutations within the core VGWPP motif of domain II, resulting in accumulation of the mutated protein and leading to defects in auxin responses (Gray et al. 2001, Ouellet et al. 2001, Reed 2001, Tian et al. 2003). Domains III and IV can mediate homo-dimerization and hetero-dimerization with other Aux/IAA family members, as well as dimerization with ARFs which also contain these two similar domains (Kim et al. 1997, Ulmasov et al. 1997, Ouellet et al. 2001). A high-throughput protein–protein interaction study of 29 Aux/IAAs and 23 ARFs in Arabidopsis showed that the majority of Aux/IAA proteins interact with themselves and with ARF activators (Vernoux et al. 2011).

Our current knowledge of the diverse roles of *Aux/IAA* genes in plant growth and development comes mainly from characterization of gain-of-function mutants in Arabidopsis (Watahiki and Yamamoto 1997, Rouse et al. 1998, Tian and Reed 1999, Fukaki et al. 2002, Yang et al. 2004) and from down-regulation in *Solanaceae* species (Wang et al. 2005, Chaabouni et al. 2009, Bassa et al. 2012, Deng et al. 2012a, Deng et al. 2012b, Su et al. 2014).

Although, several studies have found that the auxin perception and signaling machinery are important in regulating cambial activity, cambial dormancy, secondary cell wall (SCW) deposition and tension wood formation (Bhalerao and Fischer 2014), the involvement of *Aux/IAA* genes in these processes remains largely underinvestigated. Work by Nilsson et al. (2008) showed that changes in endogenous auxin levels in wood-forming tissues modulate

expression of a few key regulators such as *Aux/IAA* genes that control global gene expression patterns essential for normal secondary xylem development. Moreover, these authors found that overexpressing a stabilized version of *PttIAA3m* (mutation in the degron domain II) in *Populus* led to a reduction in cambium cell division and a decrease in secondary xylem width (Nilsson et al. 2008). To the best of our knowledge, this is the only example demonstrating the role of an *Aux/IAA* gene in xylem development in a woody species.

The sequence of the *Eucalyptus grandis* genome (Myburg et al. 2014) was published recently. This is the second forest tree genome to be sequenced, and it offers unique opportunities to analyze the characteristics of the *Aux/IAA* family in the most planted hardwood worldwide, which, in contrast to *Populus*, does not present cambium dormancy. In this study, we performed a comprehensive genome-wide identification and characterization of the *Aux/IAA* gene family in *E. grandis*. In addition to analyses of comparative phylogenetics, genomic organization and prediction of protein structural motifs, we investigated by quantitative reverse transcription–PCR (qRT–PCR) the expression profiles of the 24 *Aux/IAA* members among various organs and tissues, at different developmental stages and in response to environmental cues, with a special focus on wood-forming tissues. Based on these phylogenetic and expression results, we identified *EgrIAA4* as the best candidate gene potentially involved in the regulation of wood formation in *Eucalyptus*. Overexpression of a stabilized version of *EgrIAA4* (*EgrIAA4m*) in transgenic Arabidopsis led to auxin-related aberrant phenotypes and strongly affected interfascicular and xylary fiber formation, thereby confirming the hypothesized role of *EgrIAA4* in the regulation of cambium and wood-forming tissues.

Results

Identification and sequence analysis of the *Aux/IAA* gene family in *E. grandis*

The procedure to identify all members of the *Aux/IAA* family in *E. grandis* is illustrated in Supplementary Fig. S1. After manual curation, a total of 26 *E. grandis Aux/IAA* genes were identified. We named them according to their putative Arabidopsis orthologs (henceforth referred to as *EgrIAA* genes) based on their phylogenetic relationships (Supplementary Fig. S2). Two genes, *EgrIAA29A* and *29B*, encode protein sequences very similar to that encoded by *EgrIAA29* but both lack domains III and IV that are crucial for Aux/IAA protein activity (Supplementary Fig. S3).

The coding sequences of the vast majority (83%) of the *EgrIAA* genes are disrupted by three or four introns, and the intron positions and phases are well conserved (Fig. 1). Variations were observed for some members, however, involving mainly loss of one or more introns (*EgrIAA3A*, *19* and *33A*) and, in one case, gain of one additional intron (*EgrIAA9B*). The *EgrIAA* exon–intron patterns are similar to those of their orthologs in Arabidopsis (Supplementary Fig. S2).

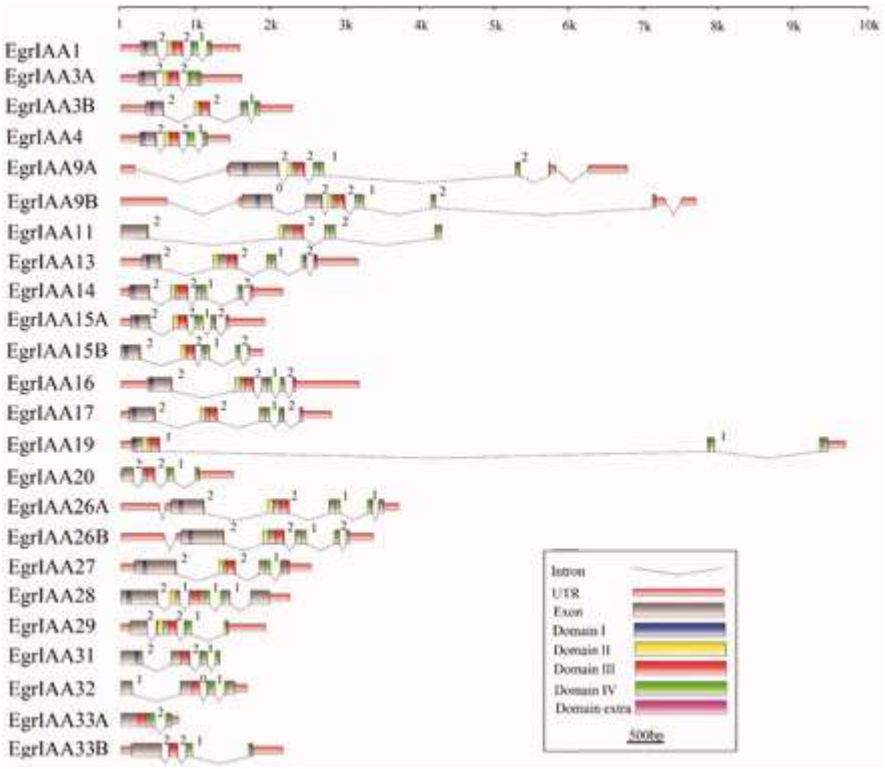

Fig. 1. Gene structures of *EgrIAA* family members. The sizes of exons and introns are indicated by the scale at the top. The protein domains are indicated by different colors. The numbers 0, 1 and 2 represent the phases of the introns.

The predicted *Egr*IAA proteins range in size from 154 (*Egr*IAA20) to 370 amino acids (*Egr*IAA26B) with corresponding molecular masses ranging from 17 to 41 kDa (Table 1). The theoretical isoelectric points also vary widely from 4.7 (*Egr*IAA33B) to 9.5 (*Egr*IAA31), indicating that they may function in different microenvironments. Pair-wise analysis of *Egr*IAA protein sequences showed that the identity levels vary greatly from 83.7% (*Egr*IAA3A and 3B) to 26.4% (*Egr*IAA9A and 28) (Supplementary Table S1). A similar wide variation of identity values was reported in Arabidopsis (Overvoorde et al. 2005) and tomato (Audran-Delalande et al. 2012). Sequence alignment of the predicted proteins and MEME protein motif analyses showed that 17 of the 24 *Egr*IAA proteins have the typical four highly conserved domains of canonical Aux/IAA proteins (Fig. 1; Supplementary Fig. S4), comprising (i) an N-terminal repressor domain I with a conserved leucine repeat motif (LxLxLx), which can recruit the co-repressor TOPLESS; (ii) a degron domain II, which is responsible for the stability of Aux/IAA proteins; and (iii) a C-terminal dimerization (CTD) domain, consisting of two highly conserved dimerization subdomains III and IV, similar to those found in ARFs (Reed 2001). Some members, however, had poorly conserved or missing domains I and/or II. For instance, the consensus sequence T/LE**L**r**L**G**L**PG in domain I is not well conserved in *Egr*IAA11, 20 and 33B, and is absent in *Egr*IAA 29, 32 and 33A (Fig. 1; Supplementary Fig. S4), and the conserved degron sequence VGWPP in domain II is not well conserved in *Egr*IAA31 (QDWPP) and is missing in *Egr*IAA20, 32, 33A and 33B (Fig. 1; Supplementary Fig. S4). Rapid degradation of Aux/IAA proteins is essential for auxin signaling, and an amino acid substitution in the degron sequence was shown to cause Aux/IAA protein accumulation leading to auxin response defects in Arabidopsis (Woodward and Bartel 2005). Therefore, the Aux/IAA proteins with either no degron sequence or a

degenerate sequence are likely to be more stable, and their molecular properties may be distinct from those of canonical Aux/IAA proteins.

Table 1. *Aux/IAA* gene family in *E. grandis*

Gene name[a]	No. of predicted alternative transcripts	Accession No.[b]	Chromosome[c]	Genome location[d]	ORF[e] (bp)	Deduced polypetide[f]			Exon No.
						Length (aa)	Mol. wt (kDa)	pI	
EgrIAA1	2	*Eucgr.K03314.1*	11	42,167,198–42,168,788	570	189	21	5.39	4
EgrIAA3A	2	*Eucgr.H03171.1*	8	46,743,317–46,744,932	612	203	23	6.02	3
EgrIAA3B	1	*Eucgr.H00216.1*	8	2,425,940–2,428,241	615	204	23	5.58	4
EgrIAA4	1	*Eucgr.H04336.1*	8	62,350,663–62,352,118	576	191	22	5.63	4
EgrIAA9A	2	*Eucgr.H02407.1*	8	32,905,397–32,912,178	1107	368	39	6.05	5
EgrIAA9B	4	*Eucgr.F02172.1*	6	29,479,509–29,487,212	1080	359	39	6.18	6
EgrIAA11[g]	1	*Eucgr.K01426.1*	11	17,332,089–17,336,565	930	309	33	5.88	4
EgrIAA13	1	*Eucgr.H02914.1*	8	42,398,802–42,401,976	801	266	29	8.8	5
EgrIAA14	1	*Eucgr.H03170.1*	8	46,720,521–46,722,685	732	243	26	6.45	5
EgrIAA15A	1	*Eucgr.J03016.1*	10	37,360,412–37,362,334	648	215	23	5.76	5
EgrIAA15B[g]	1	*Eucgr.C01083.1*	3	17,083,069–17,086,237	645	214	23	7.54	5
EgrIAA16	1	*Eucgr.H04335.1*	8	62,338,061–62,341,249	813	270	29	8.28	5
EgrIAA17[g]	1	*Eucgr.K03313.1*	11	42,152,995..42,155,812	807	268	29	6.06	5
EgrIAA19	1	*Eucgr.F02578.1*	6	35,331,299..35,341,010	585	194	22	8.33	3
EgrIAA20	1	*Eucgr.K00561.1*	11	6,262,537..6,264,036	465	154	17	4.99	4
EgrIAA26A	3	*Eucgr.F03080.1*	6	40,229,065..40,232,796	990	329	36	8.38	5
EgrIAA26B	2	*Eucgr.J02934.1*	10	36,614,769..36,618,150	1113	370	41	8.88	5
EgrIAA27	3	*Eucgr.F03050.1*	6	39,988,867..39,991,412	1050	349	37	6.27	4
EgrIAA28[g]	2	*Eucgr.C02984.1*	3	56,397,825..56,400,087	1044	347	38	6.72	5
EgrIAA29	1	*Eucgr.C01734.1*	3	29,257,063..29,258,993	651	216	25	6.6	4
EgrIAA[T]29A[h]	1	*Eucgr.C01731.1*	3	29,214,163–29,215,275	390	129	14	9.87	2
EgrIAA[T]29B[h]	1	*Eucgr.C01732.1*	3	29,230,438–29,231,106	369	122	14	9.45	2
EgrIAA31[g]	1	*Eucgr.H04141.1*	8	59,329,525–59,330,844	687	228	25	9.51	4
EgrIAA32	1	*Eucgr.B02853.1*	2	52,269,360–52,271,045	654	217	25	4.83	4
EgrIAA33A	1	*Eucgr.C02329.1*	3	43,423,640–43,424,409	531	176	19	8.71	2
EgrIAA33B	1	*Eucgr.C01373.1*	3	22,002,554–22,005,153	651	216	24	4.75	4

- [a] Designation given to *E. grandis* in this work.
- [b] Accession number in phytozome.
- [c, d] Location of the *EgrIAA* genes on the chromosome.
- [e] Length of the open reading frame in base pairs.
- [f] The number of amino acids, molecular weight (kDa) and isoelectric point (pI) of the deduced polypeptides.
- [g] Using FGENESH+ to complete the complete sequence
- [h] [T] Truncated gene.

Two types of putative nuclear localization signal (NLS) were detected in most of the *E. grandis* Aux/IAA proteins. The first has a bipartite structure comprising a conserved basic doublet, KR, between domains I and II and is associated with the presence of basic amino acids in domain II (Supplementary Fig. S4). The second one is a basic residue-rich region located in domain IV that resembles SV40-type NLSs (Supplementary Fig. S4). Most of the *Egr*IAA proteins contain both types of NLS and are therefore most probably targeted to the nucleus, consistent with their transcriptional activity. Family members such as *Egr*IAA29 and 33B, however, contain a degenerate SV40-type NLS, whereas *Egr*IAA20, *Egr*IAA32, *Egr*IAA33A and *Egr*IAA33B lack the bipartite NLS. Using transient expression assays with tomato Aux/IAA, Audran-Delalande et al. (2012) have shown that despite having a degenerate NLS, *Sl*-IAA29 protein was specifically targeted to the nucleus. In contrast, in the absence of the bipartite structure, for instance in *Sl*-IAA32, the accumulation of the protein was not restricted to the nuclear compartment (Audran-Delalande et al. 2012).

Comparative phylogenetics and chromosomal distribution of *EgrIAA* genes

The *Aux/IAA* family in *E. grandis* with only 24 members is slightly contracted compared with the 29 members in Arabidopsis and 35 in *Populus*. Its size is quite similar to that of tomato, which contains only 25 members (Table 2). To investigate the phylogenetic relationships of *Aux/IAA* family members in various species, we constructed a phylogenetic tree by using the predicted full-length amino acid sequences of Aux/IAA from *Eucalyptus*, Arabidopsis and *Populus.* The Aux/IAA members fell into 11 groups named A–K (Fig. 2); and *Egr*IAAs were distributed among all groups and had representatives even within the four groups of non-canonical Aux/IAAs (groups H, I, J and K) lacking domain I and/or II (Overvoorde et al. 2005). When compared with Arabidopsis and *Populus*, *Eucalyptus* had fewer members in each group except in group E, which notably contains two *Eucalyptus* members (*Egr*IAA15A and 15B).

Table 2. Number of *Aux/IAA* family gene members in angiosperm species

	Aux/IAA	**Reference**
Eucalyptus grandis	24	This study
Solanum lycopersicon	25	Audran-Delalande et al. (2012)
Arabidopsis thaliana	29	Overvoorde et al. (2005)
Cucumis sativus	29	Gan et al. (2013)
Populus trichocarpa	35	Kalluri et al. (2007)
Zea mays	34	Ludwig et al. (2013)
Oryza sativa	31	Jain et al. (2006)

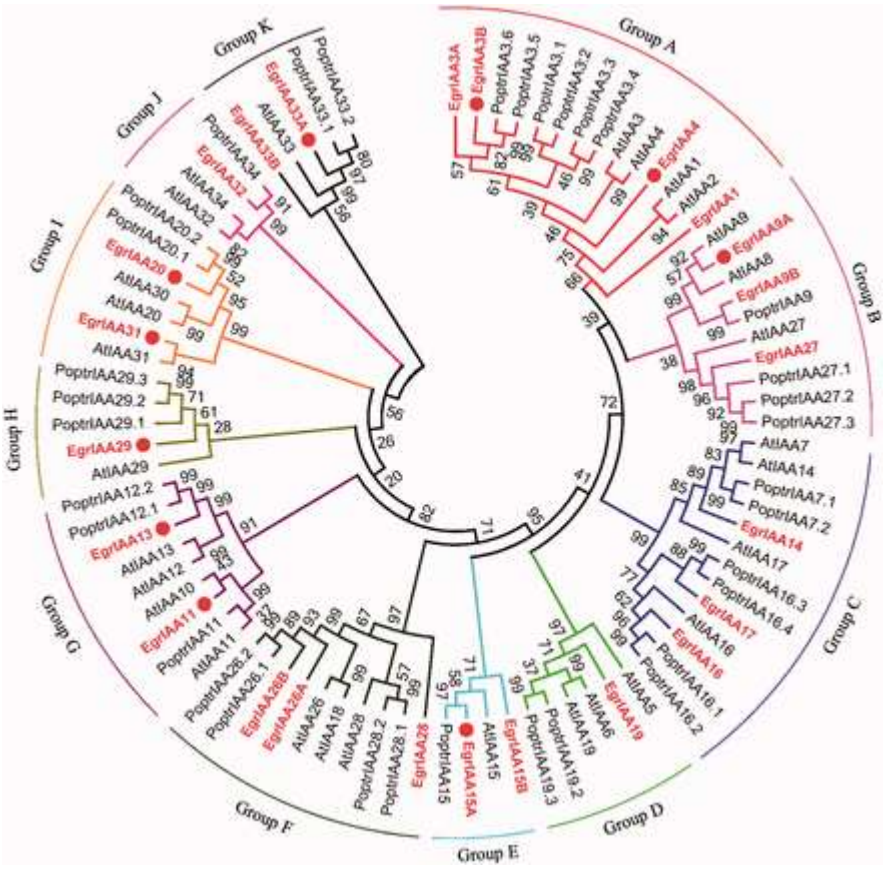

Fig. 2. Phylogenetic analysis of *Eucalyptus*, Arabidopsis and *Populus* Aux/IAA proteins. Full-length protein sequences were aligned by using the Clustal_X program. The phylogenetic tree was constructed by using the MEGA5 program and the Neighbor–Joining method with predicted Aux/IAA proteins. Bootstrap support is indicated at each node. Each Aux/IAA group (A–K) is indicated by a specific color. EgrIAAs are noted in red and bold. *EgrIAA* genes that are preferentially expressed in vascular tissue (cluster III, Fig. 3) are marked with a red solid circle.

In silico mapping of the gene loci showed that the 24 *EgrIAA* genes and the two truncated genes were unevenly distributed among six of the 11 *E. grandis* chromosomes, with 1–8 genes per chromosome; chromosomes 1, 4, 5, 7 and 9 were devoid of *Aux/IAA* genes (Table 1; Supplementary Fig. S5). Similarly, in *Populus*, the *PtrIAA* genes were present on only 10 of the 19 chromosomes, with 1–5 genes per chromosome (Kalluri et al. 2007), whereas Arabidopsis *Aux/IAA* genes were scattered on all five chromosomes (Overvoorde et al. 2005). Notably, one cluster of tandem duplicated *EgrIAA* genes was detected on chromosome 3: *EgrIAA29*, *29A* and *29B* were located within a 45 kb fragment on chromosome 3 and resulted from a recent tandem duplication event, which led to two truncated versions and probably inactive versions of *EgrIAA29* (Supplementary Fig. S3). Three pairs of *EgrIAA* genes were found to result from segmental duplications (Myburg et al. 2014) although they are located very close to each other (within a distance of <25 kb) on chromosomes 8 (*EgrIAA4/16* and *EgrIAA3A/14*) and 11 (*EgrIAA1/17*) (Supplementary Fig. S5). These six genes are phylogenetically related, the more distant genes encoding protein sequences with 61% identical residues. Members of protein pairs have identity levels higher than 63% (Supplementary Table S1), although each member of a pair belongs to a distinct phylogenetic group. *EgrIAA1*, *3A* and *4* belong to group A, whereas *EgrIAA17*, *14* and *16* belong to group C (Supplementary Figs. S2, S5). Altogether, these data suggest that one

ancestor gene underwent tandem duplication to give a first pair of *EgrIAA* genes that subsequently underwent segmental duplication events to generate the other two pairs. It seems that tandem duplication events occurred prior to the chromosomal block duplication in the *Eucalyptus Aux/IAA* family, in a similar way to the events proposed for Arabidopsis (Remington et al. 2004).

As duplication and alternative splicing are the two main mechanisms involved in diversification of function within gene families, we performed an in silico survey of the alternative transcripts predicted by the *E. grandis* genome JGI assembly v1.0, annotation v1.1 (http://www.phytozome.net/eucalyptus). Among the 24 *EgrIAA* genes, eight are predicted to have more than one splice variant (Table 1). This proportion of alternative transcripts is similar to that found in Arabidopsis. In *Eucalyptus*, most of the alternative transcripts arise from members of groups B and F, whereas in Arabidopsis the majority of them belong to groups B and G (Fig. 2; Supplementary Table S2). Some alternative transcripts are lacking domains III and/or IV (Fig. 1; Supplementary Fig. S6), probably contributing to shape the functional diversity of the family.

Expression profiling of *EgrIAA* genes in different tissues/organs and in response to environmental cues

To gain insights into the developmental patterns of expression of *EgrIAA* genes, we assessed their transcript levels by qRT–PCR in 13 different organs and tissues. The 24 *EgrIAA* genes could be detected in all the tissues tested, and most of them were preferentially expressed in certain tissues (Fig. 3). The relative transcript accumulation of all the *EgrIAA* genes is

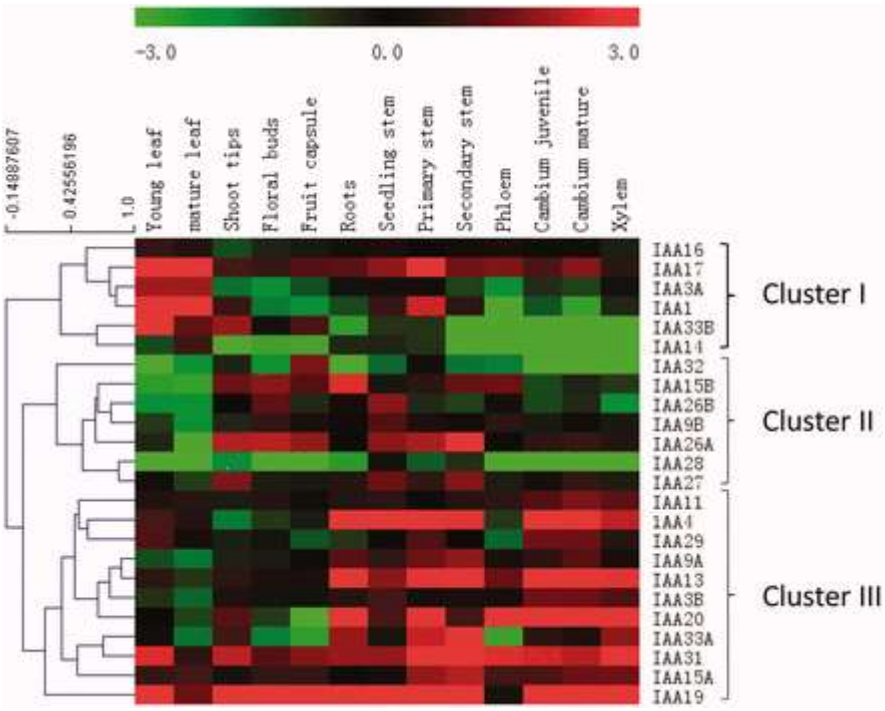

Fig. 3. Expression profiles of *EgrIAA* genes in various organs and tissues. The hierarchically clustered heat map was constructed by using the $\log_2$ ratios of relative expression values normalized to a control sample (in vitro plantlets) for 24 *EgrIAA* genes (indicated on the right) in 13 tissues and organs (indicated at the top). The genes

belonging to cluster III are preferentially expressed in vascular tissues (phloem, cambium and/or xylem) and in stems and roots.

presented as a heat map, and hierarchical clustering allowed us to group all the expression patterns into three distinct clusters (Fig. 3). Many members of the three clusters were differentially expressed in young and mature leaves. Most of them were more highly expressed in young leaves; only *EgrIAA14* was more highly expressed in mature leaves. Members of both cluster I and II were most highly expressed in non-vascular tissues, but they diverged regarding their differential expression in leaves: members of cluster I were highly expressed whereas those of cluster II were expressed at very low levels in leaves. Cluster III was the largest cluster, containing 11 members that were preferentially expressed in vascular tissues (phloem, cambium and xylem).

Within cluster III, *EgrIAA13*, *20* and *31* were relatively highly expressed in all three vascular tissues, whereas *EgrIAA4* and *33A* were expressed at higher levels in cambium and xylem than in phloem. *EgrIAA29* was preferentially expressed in cambium as compared with phloem and xylem. Most of the members of cluster III were expressed at higher levels in juvenile xylem than in mature xylem (Fig. 4A), whereas no obvious differences in their expression patterns were detected between juvenile and mature cambium (Fig. 3). Of particular note, *EgrIAA4* was the only gene that was more highly expressed in mature xylem than in juvenile xylem (Fig. 4A). Most *EgrIAA* genes from cluster III were responsive to mechanical stress due to bending (Fig. 4B). Four *EgrIAA* genes were down-regulated

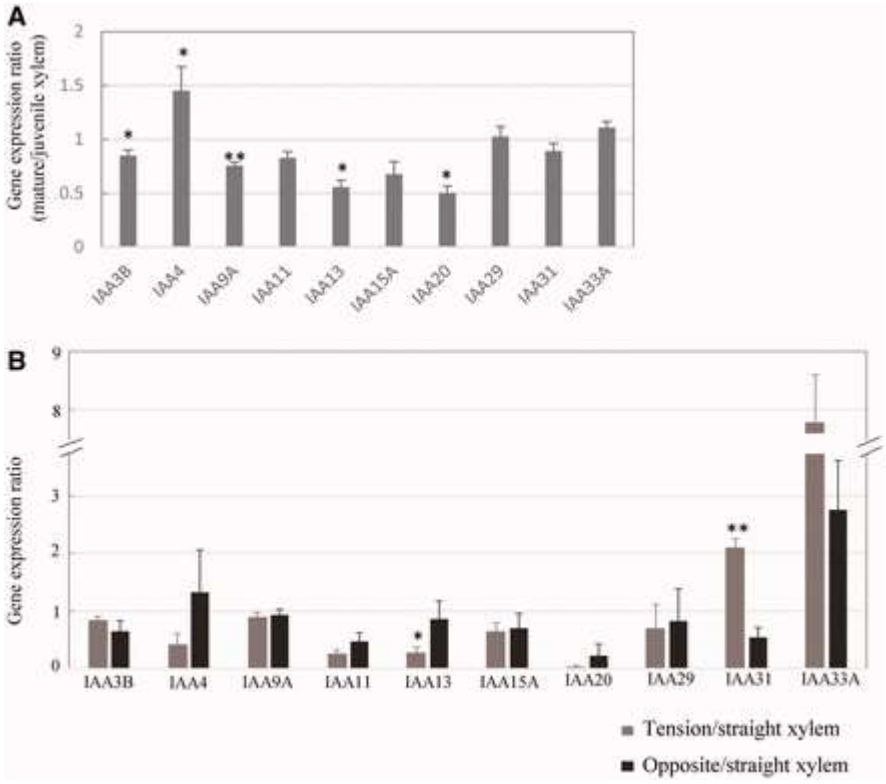

Fig. 4. Effects of developmental and environmental cues on the transcript levels of 10 *EgrIAA* genes preferentially expressed in vascular tissues. Ratios of relative mRNA abundance in (A) mature and juvenile xylem, (B) tension vs. straight xylem, and opposite vs. straight xylem. Each relative mRNA abundance was normalized to a control sample (in vitro plantlets). Error bars indicate the SE of mean expression values from

three independent experiments. Asterisks indicate values found to be significantly different (Student's *t*-test, *P*-value) **P* < 0.05; ***P* < 0.01.

(*EgrIAA4, 11*, *13* and *20*) and two (*EgrIAA31* and *33A*) were up-regulated in tension wood as compared with straight wood (Fig. 4B). Interestingly, *EgrIAA11* and *20* were down-regulated in both tension and opposite woods, whereas *EgrIAA33A* was up-regulated in these tissues (Fig. 4B).

Candidate *EgrIAA* genes potentially involved in wood formation

To identify the best candidate gene(s) potentially involved in wood formation for further functional characterization in planta, we defined several criteria: transcript abundance in vascular tissues; high expression in cambium and/or xylem and low expression in phloem; responsiveness to bending (given that the response to bending involves dramatic changes in both xylem development and SCW structure and composition); and differential expression in mature and juvenile xylem, which are known to exhibit different biochemical and physical properties. The combination of all these criteria when presented as a Venn diagram (Supplementary Fig. S7) identified *EgrIAA4* and *EgrIAA33A* as the most suitable candidates matching the first three and main criteria. Ultimately, *EgrIAA4* was selected for further functional characterization because it was the only gene that was more highly expressed in mature than in juvenile xylem (Supplementary Fig. S7).

Nuclear localization and transcriptional activity of *EgrIAA4*

When transiently expressed as a green fluorescent protein (GFP) fusion protein in BY-2 tobacco protoplasts, *Egr*IAA4 protein was located exclusively in the nucleus (Fig. 5A) as predicted by the presence of two well-conserved NLSs (Supplementary Fig. S4). The impact of *Egr*IAA4 on the transcriptional activity of target genes was assessed in tobacco protoplasts co-transfected with an effector construct expressing the full-length coding sequence of *EgrIAA4* under the 35S *Cauliflower mosaic virus* (CaMV) promoter and a reporter construct carrying DR5::GFP, an auxin-responsive promoter fused to the GFP coding sequence. The DR5::GFP reporter construct is commonly used to assess auxin-dependent transcriptional activity in planta (Ulmasov et al. 1999, Audran-Delalande et al. 2012). Basal DR5-driven GFP expression was low, but was induced up to 9-fold by exogenous auxin treatment (Fig. 5B). Co-transfection with the effector plasmid *EgrIAA4* resulted in strong repression (87%) of this auxin-induced expression of the reporter gene (Fig. 5B), indicating that *Egr*IAA4 is able to mediate an auxin response in vivo and that it functions as a strong transcriptional repressor.

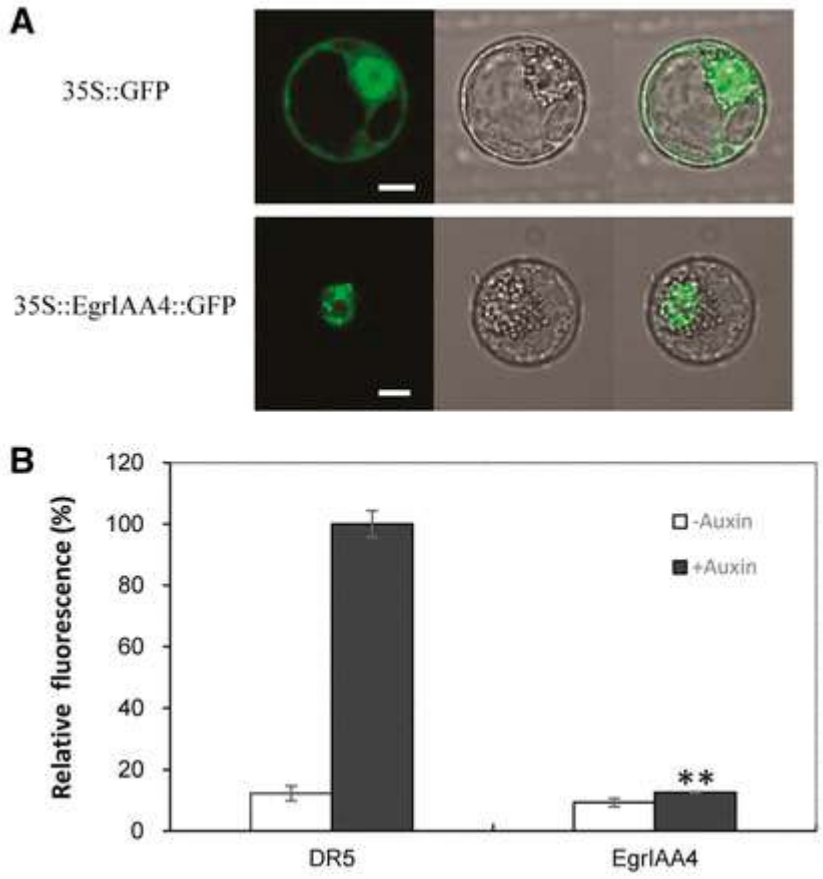

Fig. 5. Subcellular localization and repressor activity of EgrIAA4 protein on a synthetic DR5 promoter. (A) Subcellular localization of EgrIAA4–GFP fusion protein in BY-2 tobacco protoplasts. The merged images of green fluorescence (left panels) and the corresponding bright-field (middle panels) are shown in the right panels. Scale bar = 10 µm. (B) Repressor activity of EgrIAA4 protein on a synthetic DR5 promoter. Effector and reporter constructs were co-expressed in tobacco protoplasts in the presence or absence of a synthetic auxin (50 µM 2,4-D). A mock effector construct (empty vector) was used as control. In each experiment, protoplast transformations were performed in independent biological triplicates. Three independent experiments were performed and similar results were obtained; the figure indicates the data from one experiment. Error bars represent SEs of mean fluorescence. Significant statistical differences (Student's *t*-test, $P < 0.001$) from the control are marked with **.

Overexpression of *EgrIAA4m* affects plant growth and development

To gain insights into the role of *EgrIAA4*, we overexpressed in Arabidopsis a mutated version of the gene, referred to as *EgrIAA4m* (see the Materials and Methods; Supplementary Fig. S8A), encoding a stabilized form of the protein. We hypothesized that the mutation introduced in the degron domain would prevent auxin-mediated *Egr*IAA4 protein degradation. Thus *EgrIAA4m* was cloned under the control of the 35SCaMV promoter into the Gateway *pFAST-G02* expression vector and transformed into *Arabidopsis thaliana* Col-0. This *pFAST-G02* vector contains an *OLE1-GFP* selection marker that allows direct screening of transformed seeds that are fluorescent under UV light (Shimada et al. 2010). Of 10 seeds sown, six germinated giving independent *EgrIAA4m* transformants, all of similar and dramatically reduced size as compared with controls. We selected two phenotypically representative transformants (*EgrIAA4m_1.3* and *ErIAA4m_2.3*) overexpressing *EgrIAA4m* (Supplementary Fig. S8B) for further characterization. T_2 seeds from both lines germinated and half of the seedlings had the drastic phenotype, with leaf rosettes of only about 1 cm

diameter and very small, curled-down leaves that turned yellow or brown just before the plants died without flowering. (Supplementary Fig. S8C). The surviving transgenic plants (T_2) had several distinctive phenotypes in their aerial parts (Fig. 6A, B). During the seedling stage, the cotyledons were curled up, whereas the leaves were curled down and had very short petioles (Fig. 6A). During the vegetative stage, the *EgrIAA4m* transgenic plants from both lines were significantly shorter and had smaller leaf rosettes (Fig. 6B), and the inflorescence stems were thinner than those of wild-type plants. In addition, *EgrIAA4m* plants had smaller siliques and much lower fertility (i.e. no seeds or <20 seeds per plant) than wild-type plants.

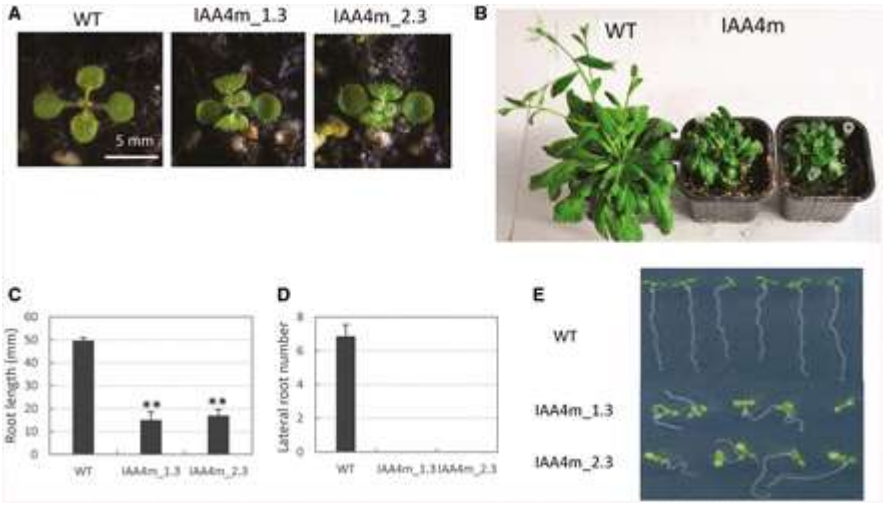

Fig. 6. Phenotypic characterization of *EgrIAA4m* transgenic plants. (A) Nine-day-old plantlets of wild-type and two representative *EgrIAA4m* lines plantlets. (B) 45-day-old wild-type and *EgrIAA4m* transgenic plants. (C, D) Primary root length and lateral root numbers in 10-day-old wild-type and *EgrIAA4m* transgenic seedlings grown on 1/2 MS medium. Error bars represent SEs of the means of primary root length ($n > 10$). Significant statistical differences (Student's *t*-test, $P < 0.001$) from the control are marked with **. (E) Three-day-old seedlings grown on vertical plates with 1/2 MS medium.

EgrIAA4m affects root development and gravitropism

To examine the root phenotype of the transgenic plants, seeds collected from T_1 plants were grown in vitro on 1/2 Murashige and Skoog (MS) medium and the primary root length and the number of lateral roots were compared 10 d after germination with those of wild-type plants. The primary roots of *EgrIAA4m* seedlings were significantly shorter (around 15 mm) than those of wild-type seedlings (around 50 mm long; Fig. 6C). In addition, no lateral roots were observed in *EgrIAA4m* transgenic seedlings, whereas wild-type seedlings had well-developed lateral roots of 6.9 mm (Fig. 6D). Seventeen days after germination, there was still no lateral root emergence in *EgrIAA4m* transgenic plants. These findings indicate that *EgrIAA4m* overexpression inhibits both primary root elongation and lateral root emergence.

The gravitropic response is a typical auxin-related phenotype, and several *Aux/IAA* Arabidopsis mutants, such as *axr5/IAA1*, *axr2/IAA7*, *slr/IAA14*, *axr3/IAA17*and *msg2/IAA19*, showed agravitropism in roots and/or hypocotyls (Watahiki and Yamamoto 1997, Rouse et al. 1998, Nagpal et al. 2000, Fukaki et al. 2002, Yang et al. 2004). To assess the gravitropic response of *EgrIAA4m* transgenic plants, we grew them on vertically oriented 1/2 MS plates.

Ten days after germination, the hypocotyls and roots of the *EgrIAA4m* transgenic plants grew in random directions (agravitropically), whereas the wild-type seedlings all grew vertically (Fig. 6E). We then returned the plates to the horizontal and checked the roots' response. After 48 h, the wild-type Arabidopsis roots had changed their growth direction by 90°, whereas the *EgrIAA4m* transgenic plants did not respond to the change in orientation (data not shown), indicating that the transgenic roots had lost their ability to perceive gravity.

EgrIAA4m negatively regulates xylem differentiation in Arabidopsis stem

Next, we investigated the impact of *EgrIAA4m* overexpression on xylem and interfascicular fiber development in Arabidopsis inflorescence stems (Fig. 7). The lignification patterns were obtained by staining stem cross-sections from plants grown for 37 d (Fig. 7A–D) or 47 d (Fig. 7E, F) with phloroglucinol-HCl. When compared with 37-day-old wild-type plants (Fig. 7A, C), the proportion of lignified tissues stained red by phloroglucinol was dramatically reduced in transgenic lines (Fig. 7B, D) suggesting that, at the same age, the activity of both fascicular and interfascicular cambium was greatly reduced and/or delayed in the transgenic plants (Fig. 7A–F). Closer examination revealed the virtual absence of lignified interfascicular

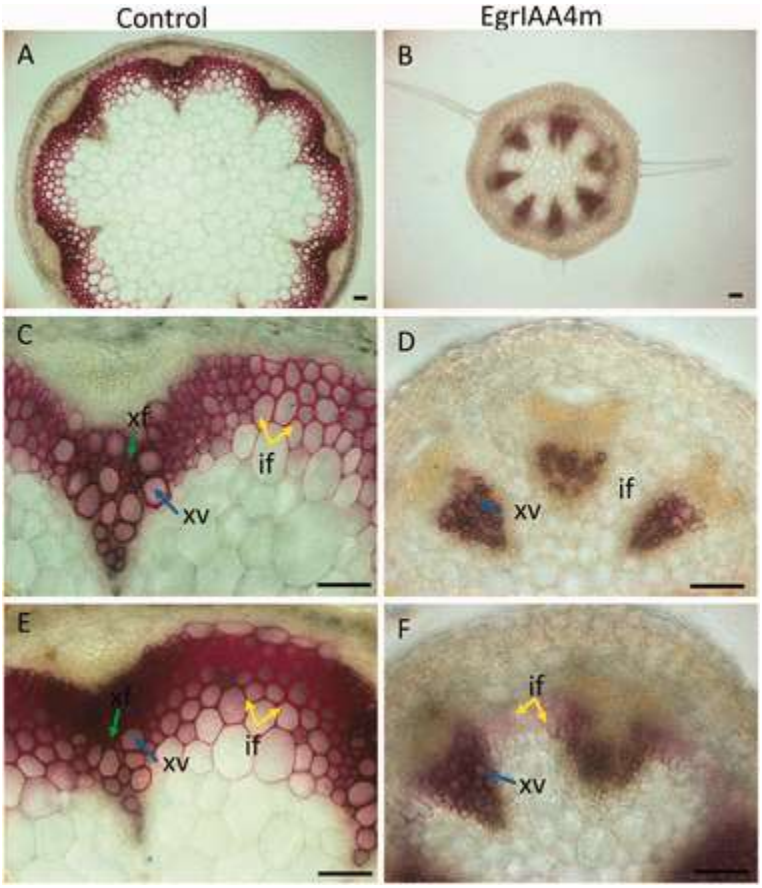

Fig. 7. Histochemical analysis of basal stem cross-sections from transgenic Arabidopsis plants expressing *EgrIAA4m*. Sections of wild-type and *EgrIAA4m* transgenic plants were stained with phloroglucinol-HCl. if, interfascicular fiber; xf, xylary fiber; xv, xylem vessel. Scale bar = 50 μm.

fibers in 37-day-old *EgrIAA4m* transgenic Arabidopsis (Fig. 7D) as compared with control (Fig. 7C). A very weak and discontinuous light reddish staining appeared in the interfascicular zone of 47-day-old transgenic plants (Fig. 7F), however, suggesting that very limited lignification had occurred. In addition, the xylem fibers in the vascular bundle regions were completely absent and the xylem vessels were much smaller than in control plants (Fig. 7C–F). These results indicate that overexpression of *EgrIAA4m* strongly and negatively affected xylem bundle and interfascicular fiber development.

Discussion

The *Aux/IAA* family in *E. grandis* contains 24 members and therefore is slightly contracted as compared with most angiosperm *Aux/IAA* families studied hitherto (Table 2). With 25 members, the gene family in tomato is the closest to *Eucalyptus* but it lacks non-canonical members in phylogenetic group I (Audran-Delalande et al. 2012), which we show here are present in *Eucalyptus*. All 11 phylogenetic groups defined in Arabidopsis are present in *Eucalyptus*, but *Eucalyptus* has fewer members in each group, except in group E, which has two members whereas Arabidopsis and *Populus* have only one member each. In Arabidopsis, transcripts of *AtIAA15*, the unique member of group E, have never been detected, suggesting that it may be a pseudogene (Remington et al. 2004). In contrast, in *E. grandis*, the transcripts of both *EgrIAA15A* and *15B* were detected by qRT–PCR, indicating they are probably functional genes. Whereas in Arabidopsis and *Populus* members of the *Aux/IAA* family arose predominantly through large-scale genomic duplication events (Remington et al. 2004, Kalluri et al. 2007), *Aux/IAA* family members in the *E. grandis* genome show evidence of only very few segmental duplication events. One cluster of recent tandem duplications was found on chromosome 3, but duplication of *EgrIAA29* led to two truncated genes lacking both domains III and IV. To the best of our knowledge, such a structure had never been reported in other species and these truncated genes are most probably not functional.

On the one hand, the virtual absence of tandem duplication in the *Eucalyptus Aux/IAA* family is especially striking because the *E. grandis* genome overall has the largest number of genes in tandem repeats reported among sequenced plant genomes (34% of the total number of genes; Myburg et al. 2014) and tandem duplication shaped functional diversity in many gene families in *Eucalyptus* such as the *MYB* (Soler et al. 2014) and *NAC* (Hussey et al. 2014) transcription factor families. On the other hand, this situation is quite similar to the *ARF* family in *E. grandis* whose size is also slightly contracted as compared with other angiosperm genomes (Yu et al. 2014). Because Aux/IAA proteins regulate auxin-mediated gene expression through interaction with ARF proteins, a corresponding dosage relationship is probably needed (Remington et al. 2004).

The expression profiles of *EgrIAA* genes in various tissues and organs showed that some have preferential expression patterns, in contrast to ARF family members that were more constitutivly expressed in the same panel of samples (Yu et al. 2014). According to the current model, Aux/IAA proteins regulate auxin-mediated gene expression by protein–protein interactions with ARFs, so the preferential expression pattern of Aux/IAA genes may

have a primary role in their physiological functions (Muto et al. 2007). All the *EgrIAA* genes in groups G, H and I were preferentially expressed in vascular tissue, and most of their orthologs in Arabidopsis and/or *Populus* also showed high/preferential expression in xylem cells (Supplementary Table S3) (Moyle et al. 2002, Kalluri et al. 2007, Hruz et al. 2008, Nilsson et al. 2008), and/or induce vascular defects in transgenic plants (Nilsson et al. 2008, Sato and Yamamoto 2008), suggesting that these phylogenetic groups regulate cambium activity and/or xylem development. Overexpression of *AtIAA20*, *30* and *31* in Arabidopsis resulted in fewer and discontinuous vascular strands in cotyledons (Sato and Yamamoto 2008). Alteration of auxin responsiveness through overexpression of a stabilized version of *PttIAA3* (the putative ortholog of *EgrIAA20*) in transgenic aspen reduced cambial cell division, caused spatial deregulation of cell division of the cambial initials and led to reductions not only in the radial but also in the axial dimensions of fibers and vessels (Nilsson et al. 2008).

Most of the *EgrIAA* genes in cluster III responded to bending stress, but their behavior seems quite different from that of their potential orthologs in *Populus* (Moyle et al. 2002). For example, *EgrIAA20* was down-regulated in tension wood, whereas its *Populus* orthologs *PttIAA3* and *4* were not affected (Moyle et al. 2002). In contrast, *EgrIAA9A* was not affected by long-term bending, whereas its *Populus* ortholog *PttIAA2* was down-regulated in tension wood (Moyle et al. 2002). In a previous study, we found that the transcript level of *EgrIAA9A* increased sharply between 6 and 24 h and then decreased between 24 h and 1 week to reach a level similar to that of the control (Paux et al. 2005). Thus *Aux/IAA* genes respond to bending in a time-dependent way, which may explain the apparent discrepancies between the responses of *Populus* and *Eucalyptus Aux/IAA* orthologs. Indeed, in our study, the plants were exposed to bending stress for 3 weeks, whereas Moyle et al. (2002) analyzed an early response to bending (from 30 min to 11 h). Indeed, our results are more consistent with those of Anderson-Gunneras et al. (2006) who analyzed *Populus* gene expression after 3 weeks bending. We found that *EgrIAA4*, *11* and *20* were all down-regulated in tension wood, as were their *Populus* orthologs (Anderson-Gunneras et al. 2006).

EgrIAA4, which belongs to subgroup A, was considered to be the best candidate to regulate cambium activity and wood formation based on its expression profile, and was chosen for functional characterization in planta. *EgrIAA4* is the ortholog of the Arabidopsis gene pair *AtIAA3* and *AtIAA4*. Only the function of *AtIAA3* has been studied through gain-of-function experiments. The *AtIAA3* mutation *shy2* produces plants with shorter hypocotyls, fewer lateral roots and a slower gravitropic response than the wild type (Reed et al. 1998, Tian and Reed 1999). *AtIAA3* was shown recently to be part of the auxin signaling module (SLR/IAA14–ARF7–ARF19 and SHY2/IAA3–ARFs) regulating lateral root formation (Goh et al. 2012). Likewise the down-regulation of *Sl-IAA3*, the ortholog of *AtIAA3* in tomato, leads to reduced growth of primary roots and inhibition of lateral roots (Chaabouni et al. 2009). Overexpression of an auxin-insensitive version of *EgrIAA4* in Arabidopsis led to very similar but more severe aberrant auxin response phenotypes. The gravitropic response was lost completely, and growth and development were severely affected, with much reduced height and diameter of the inflorescence stem, reduced leaf size and fertility, and absence of lateral roots. Notably, *EgrIAA4m* overexpression also led to phenotypic alterations of the vascular system not reported yet for its Arabidopsis ortholog. The development of both xylem and interfascicular fibers was dramatically delayed and reduced, suggesting reduced

cambium activity in response to the altered auxin responsiveness induced by *EgrIAA4m* expression. The lignified secondary walls of the interfascicular fibers appeared very late, whereas that of the xylary fibers was virtually undetectable. This phenotype, together with the expression pattern of *EgrIAA4*, strongly suggests that auxin signaling and EgrIAA4 are important in fiber development and SCW deposition.

Materials and Methods

Identification of *Aux/IAA* genes in *Eucalyptus*

We used 29 Arabidopsis Aux/IAA protein sequences and BLASTP to search for related proteins predicted by the *E. grandis* genome (JGI assembly v1.0, annotation v1.1, http://www.phytozome.net/eucalyptus), which identified 55 potential *E. grandis* Aux/IAA proteins. Then, we used the Pfam database (http://pfam.sanger.ac.uk/search) and NCBI conserved domain database (http://www.ncbi.nlm.nih.gov/cdd) web server to examine the conserved domains (Finn et al. 2010, Marchler-Bauer et al. 2011). The incomplete gene models were completed by FGENESH+ (http://linux1.softberry.com), and redundant and invalid gene models were removed. The corrected *E. grandis* Aux/IAA protein sequences were used as query sequences in two subsequent searches: first, a BLASTP search of the *E. grandis* proteome for exhaustive identification of divergent *E. grandis* gene family members, and, secondly, TBLASTN searches of the *E. grandis* genome for any possible unpredicted genes. In total, 26 *EgrIAA* genes were identified in the *E. grandis* genome (*E. grandis* genome V1.1, May 2012). For validation, we also used *Populus* Aux/IAA proteins as queries in the complete search procedure described above, and we obtained exactly the same final 26 *EgrAux/IAA* genes. Gene information on chromosomal location was retrieved from the *E. grandis* genome browser (http://www.phytozome.net/eucalyptus) with manual curation, and we mapped their loci using MapChart 2.2 (Voorrips 2002). Basic physical and chemical parameters of Aux/IAA proteins were calculated by means of the online ProtParam tool (http://web.expasy.org/protparam/).

Sequence, gene structure and phylogenetic analysis

Conserved protein motifs of *Egr*IAA were determined by use of MEME-MAST programs (http://meme.sdsc.edu/meme) (Bailey et al. 2009). The exon–intron structures were extracted from Phytozome with manual curation and visualized by Fancy Gene v1.4 (http://bio.ieo.eu/fancygene/). Multiple protein sequence alignments was performed by using the Clustal_X2 program (Version 2.0.11). All predicted protein sequences were used for phylogenetic analysis, and the phylogenetic trees were constructed with the MEGA5 program by using the Neighbor–Joining method with 1,000 bootstrap.

Plant materials and growth conditions

The provenance and preparation of all *Eucalyptus* organs and tissues were as described in Cassan-Wang et al. (2012). *Arabidopsis thaliana* ecotype Col-0 plants were grown in a growth chamber under the conditions: 16 h day : 8 h night for long days, 22 : 20°C day :

night temperature, 70% relative humidity, 200 µmol photons m^{-1} s^{-1} light intensity (intense luminosity). The plants were watered every 2 d and fertilized weekly. Seeds were surface-sterilized for 1 min in 70% ethanol, 10 min in 25% bleach, rinsed five times in sterile water and plated on MS medium containing 1.0% sucrose solidified with 1% agar.

RNA isolation, cDNA synthesis and qRT–PCR

Total RNAs were extracted from 100–200 mg of frozen material as described previously (Southerton et al. 1998), and genomic DNA contamination was removed by using the Turbo DNA-*free*™ kit (Ambion). RNA concentrations and purity were determined by using a NanoDrop spectrophotometer ND-1000 (Thermo Scientific), and integrity was assessed by using the Agilent 2100 Bioanalyzer. Only samples with RNA integrity number (RIN) >7 were used for reverse transcription. cDNA was reversed transcribed from 2 µg of total RNA using the High Capacity cDNA Reverse Transcription Kit (Applied Biosystems).

Primers were designed by using the software QuantPrime (qPCR primer design tool: http://www.quantprime.de/; Arvidsson et al. 2008); the sequences are shown in Supplementary Table S4. Oligonucleotides were synthesized by Sigma Life Science. qRT–PCR was performed by the Genotoul service in Toulouse (http://genomique.genotoul.fr/) using BioMark® 96:96 Dynamic Array integrated fluidic circuits (Fluidigm Corporation) as described previously (Cassan-Wang et al. 2012). Only primers that produced linear amplification and qPCR products with single-peak melting curves were used for further analysis. The efficiency of each pair of primers was determined from the data of the amplification Ct value plot with a serial dilution of mixture cDNA and the equation $E = 10^{(-1/\text{slope})} - 1$. The $E^{-\Delta\Delta Ct}$ method was used to calculate relative mRNA fold change compared with a control sample by using the formula $(E_{\text{target}})^{\Delta Ct\_\text{target (control−sample)}}/(E_{\text{reference}})^{\Delta Ct\_\text{reference (control−sample)}}$ (Pfaffl 2001), and five reference genes (IDH, PP2A1, PP2A3, EF-1a and SAND, Supplementary Table S4) were used for data normalization. In vitro plantlets were used as control samples.

***EgrIAA4* amplification and gain-of-function transgenic Arabidopsis construction**

The *EgrIAA4* gene was amplified by PCR using Phusion Taq (Thermo) and a gene-specific primer pair: 5′-CACCATGGCAGCTCAAGGAGAGGAT-3′ and 5′-AACCTCTGATGACCCTTTCATGATT-3′ based on sequence prediction from the *E. grandis* genome v.1.1 (Eucgr.H04336.1). To investigate the function of this gene, we created a mutation in the auxin degradation domain by changing the codon for amino acid residue 80 from one that encodes proline to one that encodes serine (P-to-S) in domain II by using overlap PCR. The overlap primers were 5′-**ATC**GGACCGGACTCCACCCCACGACTTGTGCCTTA-3′ and 5′-CGTGGGGTGG**AGT**CCGGTCCGATCCTACCGAAA-3′. The underlined sequences indicate the overlap region and the bold bases are the mutated nucleotides. The *EgrIAA4m* fragment was cloned into the *pENTR/D-TOPO* vector (Invitrogen) for sequencing. After sequencing, we recombined the *EgrIAA4m* fragment into the destination vector *pFAST-G02* by using LR Clonase (Invitrogen). The vector pFAST-*EgIAA4m* was transformed into *Agrobacterium tumefaciens* strain GV3101, and then transformed into *A. thaliana* ecotype Col-0 by using the floral dip method (Clough and Bent 1998).

Transient gene expression in protoplasts

Protoplasts for transfection were obtained from suspension-cultured tobacco (*Nicotiana tabacum*) BY-2 cells according to the method of Leclercq et al. (2005). They were transfected by a modified polyethylene glycol method as described by Abel and Theologis (1994). To study the nuclear localization of selected Aux/IAAs, 'effector' constructs were created by fusing full-length cDNAs in-frame with the *GFP* sequence to produce a fusion protein at the C-terminus of GFP and under the control of the 35SCaMV promoter in the vector *pK7FWG2.0* (Karimi et al. 2002). Transfected protoplasts were incubated for 16 h at 25°C and examined for GFP florescence by using a Leica TCS SP2 laser scanning confocal microscope. Images were obtained with a ×40 water-immersion objective. For co-transfection assays, the full-length cDNAs encoding selected Aux/IAA proteins were cloned under the control of the 35SCaMV promoter in the vector pGreen. The 'reporter' constructs used a synthetic auxin-responsive promoter DR5 fused to the *GFP* reporter gene. Tobacco BY-2 protoplasts were co-transfected with the reporter and effector constructs as described in Audran-Delalande et al. (2012). After 16 h incubation, GFP expression was quantified by flow cytometry (LSR Fortessa, BD Bioscience), and the data were analyzed using BD CellQuest and BD FacsDiva software. Transfection assays were performed with three independent replicates, and 3,000–4,000 protoplasts were gated for each sample. GFP fluorescence corresponds to the average fluorescence intensity of the protoplast population after subtraction of autofluorescence determined with non-transformed protoplasts. 2,4-D (50 µM) was used for auxin treatment.

Microscopy analysis

Arabidopsis hypocotyls and the basal ~1 cm of inflorescence stems were harvested from 37- and 47-day-old plants, and stored in 70% ethanol. Sections were prepared by using a vibratome Leica VT1000 S. Lignin polymers are the characteristic components of SCW and are normally absent from primary cell walls; therefore, we used lignin deposition detection techniques to screen for SCW phenotype. Cross-sections of inflorescence stem and hypocotyl (~80 µm thick) were stained with phloroglucinol-HCl, which stains violet-red specifically the lignin polymer precursors coniferaldehyde and *p*-coumaraldehyde in the SCW. Phloroglucinol-HCl was directly applied on the slide and images were recorded with a CCD camera (Photonic Science; http://www.photonic-science.co.uk).

Funding

This work was supported by the Centre National pour la Recherche Scientifique (CNRS); the University Paul Sabatier Toulouse III (UPS); the Agence Nationale de la Recherche (ANR); the French Laboratory of Excellence [project 'TULIP' (ANR-10-LABX-41; ANR-11-IDEX-0002-02)]; the Plant KBBE TreeForJoules [project ANR-2010-KBBE-007-01 (FR) and P-KBBE/AGR_GPL/0001/2010 (FCT, PT) and the project microEGo (PTDC/AGR-GPL/098179/2008; FCT, PT); the China Scholarship Council [a PhD grant to H.Y.]; the Departament d'Universitats, Recerca i Societat de la Informació de la Generalitat de Catalunya [a post-doctoral fellowship 'Beatriu de Pinós' to M.S.]; the Fundação para a

Ciência e a Tecnologia (FCT) [a research contract from the Ciência 2008 program and a post-doctoral fellowship SFRH/BPD/92207/2013 to J.A.P.P.].

Previous SectionNext Section

Disclosures

The authors have no conflicts of interest to declare.

Previous SectionNext Section

Acknowledgments

The authors are grateful to C. Dunand and Q. Li for their help with the bioinformatics analysis, to E. Camargo, J.M. Gion and E. Villar (CIRAD, FR), F. Melun and L. Harvengt (FCBA, France), C. Araujo and L. Neves (AltriFlorestal, Portugal) and C. Marques (RAIZ, Portugal) for kindly providing and/or allowing collection of *Eucalyptus* organ and tissue samples, to C. Graça and N. Saidi for help with sample collection and RNA extraction, and to N. Ladouce and V. Carocha for performing qRT–PCR. Thanks to the Bioinfo Genotoul Platform (http://bioinfo.genotoul.fr) for access to resources and to the Genome and Transcriptome Platform (http://get.genotoul.fr/) for advice and technical assistance with high-throughput Biomark Fluidigm, to Y. Martinez (FR3450) for assistance with microscopy (Plateforme Imagerie TRI; http://tri.ups-tlse.fr/), and to C. Pecher and A. Zakaroff-Girard for their technical assistance and expertise in flow cytometry (Cytometry and Cell Sorting Platform, INSERM UPS UMR 1048, Toulouse RIO imaging platform).

Abbreviations

AFB
: auxin signaling F-box

ARF
: auxin-response factor

AuxRE
: auxin-responsive *cis*-element

Aux/IAA
: auxin/indole-3-acetic acid

CaMV
: *Cauliflower mosaic virus*

EAR
: ethylene-responsive element-binding factor-associated amphiphilic repression

GFP
: green fluorescent protein

MS
: Murashige and Skoog

NLS
: nuclear localization signal

qRT–PCR
: quantitative reverse transcription–PCR

SCW
: secondary cell wall

TIR1
: transport inhibitor response1

References

Abel S, Theologis A. Transient transformation of *Arabidopsis* leaf protoplasts: a versatile experimental system to study gene expression. *Plant J.* 1994;5:421-427.

Ainley WM, Walker JC, Nagao RT, Key JL. Sequence and characterization of two auxin-regulated genes from soybean. *J. Biol. Chem.* 1988;263:10658-10666.

Andersson-Gunneras S, Mellerowicz EJ, Love J, Segerman B, Ohmiya Y, Coutinho PM, et al. Biosynthesis of cellulose-enriched tension wood in *Populus*: global analysis of transcripts and metabolites identifies biochemical and developmental regulators in secondary wall biosynthesis. *Plant J.* 2006;45:144-165.

Arvidsson S, Kwasniewski M, Riano-Pachon DM, Mueller-Roeber B. QuantPrime—a flexible tool for reliable high-throughput primer design for quantitative PCR. *BMC Bioinformatics* 2008;9:465.

Audran-Delalande C, Bassa C, Mila I, Regad F, Zouine M, Bouzayen M. Genome-wide identification, functional analysis and expression profiling of the Aux/IAA gene family in tomato. *Plant Cell Physiol.* 2012;53:659-672.

Baba K, Karlberg A, Schmidt J, Schrader J, Hvidsten TR, Bako L, et al. Activity–dormancy transition in the cambial meristem involves stage-specific modulation of auxin response in hybrid aspen. *Proc. Natl Acad. Sci. USA* 2011;108:3418-3423.

Bailey TL, Boden M, Buske FA, Frith M, Grant CE, Clementi L, et al. MEME SUITE: tools for motif discovery and searching. *Nucleic Acids Res.* 2009;37:W202-W208.

Bassa C, Mila I, Bouzayen M, Audran-Delalande C. Phenotypes associated with down-regulation of Sl-IAA27 support functional diversity among Aux/IAA family members in the tomato. *Plant Cell Physiol.*

Bhalerao RP, Fischer U. Auxin gradients across wood—instructive or incidental? *Physiol. Plant.* 2014;151:43-51.

Calderon Villalobos LI, Lee S, De Oliveira C, Ivetac A, Brandt W, Armitage L, et al. A combinatorial TIR1/AFB–Aux/IAA co-receptor system for differential sensing of auxin. *Nat. Chem. Biol.* 2012;8:477-485.

Cassan-Wang H, Soler M, Yu H, Camargo EL, Carocha V, Ladouce N, et al. Reference genes for high-throughput quantitative reverse transcription–PCR analysis of gene expression in organs and tissues of *Eucalyptus* grown in various environmental conditions. *Plant Cell Physiol.* 2012;53:2101-2116.

Chaabouni S, Jones B, Delalande C, Wang H, Li Z, Mila I, et al. Sl-IAA3, a tomato Aux/IAA at the crossroads of auxin and ethylene signalling involved in differential growt*h. J. Exp. Bot. 2009;*60:1349-1362.

Clough SJ, Bent AF. Floral dip: a simplified method for Agrobacterium-mediated transformation of *Arabidopsis thaliana. Plant J*. 1998;16:735-743.

Deng W, Yan F, Liu M, Wang X, Li Z. Down-regulation of SlIAA15 in tomato altered stem xylem development and production of volatile compounds in leaf exudates. *Plant Signal. Behav.* 2012a;7:911-913.

Deng W, Yang Y, Ren Z, Audran-Delalande C, Mila I, Wang X, et al. The tomato SlIAA15 is involved in trichome formation and axillary shoot development. *New Phytol.* 2012b;194:379-390.

Dharmasiri N, Dharmasiri S, Estelle M. The F-box protein TIR1 is an auxin receptor. *Nature 2005;*435:441-445.

Finn RD, Mistry J, Tate J, Coggill P, Heger A, Pollington JE, et al. The Pfam protein families database. *Nucleic Acids Res*. 2010;38:D211-D222.

Friml J. Auxin transport—shaping the plant. *Curr. Opin. Plant Biol.*

Fukaki H, Tameda S, Masuda H, Tasaka M. Lateral root formation is blocked by a gain-of-function mutation in the SOLITARY-ROOT/IAA14 gene of *Arabidopsis. Plant J.* 2002;29:153-*168.*

Gan D, Zhuang D, Ding F, Yu Z, Zhao Y. Identification and expression analysis of primary auxin-responsive Aux/IAA gene family in cucumber (Cucumis sativus). *J. Genet.* 2013;92:513-21.

Goh T, Kasahara H, Mimura T, Kamiya Y, Fukaki H. Multiple AUX/IAA–ARF modules regulate lateral root formation: the role of Arabidopsis SHY2/IAA3-mediated auxin signalling. *Philos. Trans. R. Soc. B: Biol. Sci.* 2012;367:1461-1468.

Gray WM, Kepinski S, Rouse D, Leyser O, Estelle M. Auxin regulates SCF(TIR1)-dependent degradation of AUX/IAA proteins. *Nature* 2001;414:271-276.

Guilfoyle TJ, Hagen G. Auxin response factors. *Curr. Opin. Plant Biol.* 2007;10:453-460.

Hellgren JM, Olofsson K, Sundberg B. Patterns of auxin distribution during gravitational induction of reaction wood in poplar and pine. *Plant Physiol.* 2004;135:212-220.

Hruz T, Laule O, Szabo G, Wessendorp F, Bleuler S, Oertle L, et al. Genevestigator v3: a reference expression database for the meta-analysis of transcriptomes. *Adv. Bioinformatics.* 2008;2008:420747.

Hussey SG, Saïdi MN, Hefer CA, Myburg AA, Grima-Pettenati . Structural, evolutionary and functional analysis of the NAC domain protein family in *Eucalyptus. New Phytol.* 2014. (in press).

Jain M, Kaur N, Garg R, Thakur JK, Tyagi AK, Khurana JP. Structure and expression analysis of early auxin-responsive Aux/IAA gene family in rice (Oryza sativa). *Funct. Integr. Genomics* 2006;6:47-59.

Kalluri UC, Difazio SP, Brunner AM, Tuskan GA. Genome-wide analysis of Aux/IAA and ARF gene families in *Populus trichocarpa. BMC Plant Biol.* 2007;7:59.

Karimi M, Inze D, Depicker A. GATEWAY vectors for Agrobacterium-mediated plant transformation. *Trends Plant Sci.* 2002;7:193-195.

Kepinski S, Leyser O. The Arabidopsis F-box protein TIR1 is an auxin receptor. *Nature* 2005;435:446-451.

Kim J, Harter K, Theologis A. Protein–protein interactions among the Aux/IAA proteins. *Proc. Natl Acad. Sci. USA* 1997;94:11786-11791.

Leclercq J, Ranty B, Sanchez-Ballesta MT, Li Z, Jones B, Jauneau A, et al. Molecular and biochemical characterization of LeCRK1, a ripening-associated tomato CDPK-related kinase. *J. Exp. Bot.* 2005;56:25-35.

Ludwig Y, Zhang Y, Hochholdinger F. The maize *(Zea mays L.) AUXIN/INDOLE-3-ACETIC ACID* gene family: phylogeny, synteny, and unique root-type and tissue-specific expression patterns during development. *PLoS One* 2013;8:e78859.

Marchler-Bauer A, Lu S, Anderson JB, Chitsaz F, Derbyshire MK, DeWeese-Scott C, et al. CDD: a Conserved Domain Database for the functional annotation of proteins. *Nucleic Acids Res*. 2011;39:D225-D229.

Mellerowicz EJ, Baucher M, Sundberg B, Boerjan W. Unravelling cell wall formation in the woody dicot stem. *Plant Mol. Biol.* 2001;47:239-274.

Miyashima S, Sebastian J, Lee JY, Helariutta Y. Stem cell function during plant vascular development. *EMBO J.* 2013;32:178-193.

Mockaitis K, Estelle M. Auxin receptors and plant development: a new signaling paradigm. *Annu. Rev. Cell Dev. Biol.* 2008;24:55-80.

Morey PR, Cronshaw J. Induction of tension wood by 2,4-dinitrophenol and auxins. *Protoplasma* 1968;65:393-405.

Moyle R, Schrader J, Stenberg A, Olsson O, Saxena S, Sandberg G, et al. Environmental and auxin regulation of wood formation involves members of the Aux/IAA gene family in hybrid aspen. *Plant J.* 2002;31:675-685.

Muto H, Watahiki MK, Nakamoto D, Kinjo M, Yamamoto KT. Specificity and similarity of functions of the Aux/IAA genes in auxin signaling of Arabidopsis revealed by promoter-exchange experiments among MSG2/IAA19, AXR2/IAA7, and SLR/IAA14. *Plant Physiol. 2007;*144:187-196.

Myburg AA, Grattapaglia D, Tuskan GA, Hellsten U, Hayes RD, Grimwood J, et al. The genome of *Eucalyptus grandis. Nature* 2014;509:356-362.

Nagpal P, Walker LM, Young JC, Sonawala A, Timpte C, Estelle M, et al. AXR2 encodes a member of the Aux/IAA protein family. *Plant Physiol.* 2000;123:563-574.

Nilsson J, Karlberg A, Antti H, Lopez-Vernaza M, Mellerowicz E, Perrot-Rechenmann C, et al. Dissecting the molecular basis of the regulation of wood formation by auxin in hybrid aspen. *Plant Cell* 2008;20:843-855.

Ouellet F, Overvoorde PJ, Theologis A. IAA17/AXR3: biochemical insight into an auxin mutant phenotype. *Plant Cell* 2001;13:829-841.

Overvoorde PJ, Okushima Y, Alonso JM, Chan A, Chang C, Ecker JR, et al. Functional genomic analysis of the AUXIN/INDOLE-3-ACETIC ACID gene family members in *Arabidopsis thaliana. Plant Cell* 2005;17:3282-3300.

Paux E, Carocha V, Marques C, Mendes de Sousa A, Borralho N, Sivadon P, et al. Transcript profiling of *Eucalyptus xylem* genes during tension wood formation. *New Phytol.* 2005;167:89-100.

Pfaffl MW. A new mathematical model for relative quantification in real-time RT–PCR. *Nucleic Acids Res.* 2001;29:e45.

Pilate G, Déjardin A, Laurans F, Leplé JC. Tension wood as a model for functional genomics of wood formation. *New Phytol.* 2004;164:63-72.

Plomion C, Leprovost G, Stokes A. Wood formation in trees. *Plant Physiol.* 2001;127:1513-1523.

Reed JW. Roles and activities of Aux/IAA proteins in *Arabidopsis. Trends Plant Sci.* 2001;6:420-425.

Reed JW, Elumalai RP, Chory J. Suppressors of an *Arabidopsis thaliana* phyB mutation identify genes that control light signaling and hypocotyl elongation. *Genetics* 1998;148:1295-1310.

Remington DL, Vision TJ, Guilfoyle TJ, Reed JW. Contrasting modes of diversification in the Aux/IAA and ARF gene families. *Plant Physiol.* 2004;135:1738-1752.

Rouse D, Mackay P, Stirnberg P, Estelle M, Leyser O. Changes in auxin response from mutations in an AUX/IAA gene. *Science* 1998;279:1371-1373.

Sato A, Yamamoto KT. Overexpression of the non-canonical Aux/IAA genes causes auxin-related aberrant phenotypes in *Arabidopsis. Physiol. Plant.* 2008;133:397-405.

Schrader J, Baba K, May ST, Palme K, Bennett M, Bhalerao RP, et al. Polar auxin transport in the wood-forming tissues of hybrid aspen is under simultaneous control of developmental and environmental signals. *Proc. Natl Acad. Sci. USA* 2003;100:10096-10101.

Schrader J, Moyle R, Bhalerao R, Hertzberg M, Lundeberg J, Nilsson P, et al. Cambial meristem dormancy in trees involves extensive remodelling of the transcriptome. *Plant J.* 2004;40:173-187.

Shimada TL, Shimada T, Hara-Nishimura I. A rapid and non-destructive screenable marker, FAST, for identifying transformed seeds of *Arabidopsis thaliana. Plant J.* 2010;61:519-528.

Soler M, Camargo ELO, Carocha V, Cassan-Wang H, San Clemente H, Savelli B, et al. The *Eucalyptus grandis* R2R3-MYB transcription factor family: evidence for woody growth related evolution and function. *New Phytol.* 2014. (in press).

Southerton SG, Marshall H, Mouradov A, Teasdale RD. *Eucalypt* MADS-box genes expressed in developing flowers. *Plant Physiol.* 1998;118:365-372.

Su L, Bassa C, Audran C, Cheniclet C, Chevalier C, Bouzayen M, et al. The auxin Sl-IAA17 transcriptional repressor controls fruit size via the regulation of endoreduplication-related cell expansion. *Plant Cell Physiol.* 2014;55:1969-1976.

Sundberg B, Uggla C, Tuominen H. Cambial growth and auxin gradients. In: Savidge RA, Barnett JR, Napier R, editors. *Cell and Molecular Biology of Wood Formation.* Oxford: BIOS Scientific Publishers; 2000. p. 169-188.

Szemenyei H, Hannon M, Long JA. TOPLESS mediates auxin-dependent transcriptional repression during *Arabidopsis embryogenesis. Science* 2008;319:1384-1386.

Tan X, Calderon-Villalobos LI, Sharon M, Zheng C, Robinson CV, Estelle M, et al. Mechanism of auxin perception by the TIR1 ubiquitin ligase. *Nature* 2007;446:640-645.

Theologis A, Huynh TV, Davis RW. Rapid induction of specific mRNAs by auxin in pea epicotyl tissue. *J. Mol. Biol.* 1985;183:53-68.

Tian Q, Nagpal P, Reed JW. Regulation of *Arabidopsis* SHY2/IAA3 protein turnover. *Plant J.* 2003;36:643-651.

Tian Q, Reed JW. Control of auxin-regulated root development by the *Arabidopsis thaliana* SHY2/IAA3 gene. *Development* 1999;126:711-721.

Timell T. The chemical composition of tension wood. *Svensk Papperstidning* 1969;72:173-181.

Tiwari SB, Hagen G, Guilfoyle TJ. Aux/IAA proteins contain a potent transcriptional repression domain. *Plant Cell* 2004;16:533-543.

Tuominen H, Puech L, Fink S, Sundberg B. A radial concentration gradient of indole-3-acetic acid is related to secondary xylem development in Hybrid Aspen. *Plant Physiol.* 1997;115:577-585.

Uggla C, Magel E, Moritz T, Sundberg B. Function and dynamics of auxin and carbohydrates during earlywood/latewood transition in scots pine. *Plant Physiol.* 2001;125:2029-2039.

Uggla C, Mellerowicz EJ, Sundberg B. Indole-3-acetic acid controls cambial growth in scots pine by positional signaling. *Plant Physiol.* 1998;117:113-121.

Uggla C, Moritz T, Sandberg G, Sundberg B. *Auxin* as a positional signal in pattern formation in plants. *Proc. Natl Acad. Sci. USA* 1996;93:9282-9286.

Ulmasov T, Hagen G, Guilfoyle TJ. Activation and repression of transcription by auxin-response factors. *Proc. Natl Acad. Sci. USA* 1999;96:5844-5849.

Ulmasov T, Murfett J, Hagen G, Guilfoyle TJ. Aux/IAA proteins repress expression of reporter genes containing natural and highly active synthetic auxin response elements. *Plant Cell* 1997;9:1963-1971.

Vernoux T, Brunoud G, Farcot E, Morin V, Van den Daele H, Legrand J, et al. The auxin signalling network translates dynamic input into robust patterning at the shoot apex. *Mol. Syst. Biol.* 2011;7:508.

Voorrips RE. MapChart: software for the graphical presentation of linkage maps and QTLs. *J. Hered*. 2002;93:77-78.

Walker JC, Key JL. Isolation of cloned cDNAs to auxin-responsive poly(A)RNAs of elongating soybean hypocotyl. *Proc. Natl Acad. Sci. USA* 1982;79:7185-7189.

Wang H, Jones B, Li Z, Frasse P, Delalande C, Regad F, et al. The tomato Aux/IAA transcription factor IAA9 is involved in fruit development and leaf morphogenesis. *Plant Cell* 2005;17:2676-2692.

Watahiki MK, Yamamoto KT. The massugu1 mutation of *Arabidopsis* identified with failure of auxin-induced growth curvature of hypocotyl confers auxin insensitivity to hypocotyl and leaf. *Plant Physiol.* 1997;115:419-426.

Woodward AW, Bartel B. Auxin: regulation, action, and interaction. *Ann. Bot.* 2005;95:707-735.

Yang X, Lee S, So JH, Dharmasiri S, Dharmasiri N, Ge L, et al. The IAA1 protein is encoded by AXR5 and is a substrate of SCF(TIR1*). Plant J.* 2004;40:772-782.

Yu H, Soler M, Mila I, San Clemente H, Savelli B, Dunand C, et al. Genome-wide characterization and expression profiling of the AUXIN RESPONSE FACTOR (ARF) gene family in *Eucalyptus grandis. PLoS One* 2014;9:e108906.